Journal of Renewable Materials

Tech Science Press

DOI: 10.32604/jrm.2023.029308

ARTICLE

A Circular Economy Use of Post-Consumer Polypropylene Packaging for Low Thermal Conductive and Fire-Retardant Building Material Applications

Jakkid Sanetuntikul[1], Borwon Narupai[2] and Nawadon Petchwattana[3,*]

[1]Faculty of Engineering and Technology, King Mongkut's University of Technology North Bangkok, Rayong, 21120, Thailand

[2]Expert Center of Innovative Materials, Thailand Institute of Scientific and Technological Research, Pathum Thani, 12120, Thailand

[3]Department of Chemical Engineering, Faculty of Engineering, Srinakharinwirot University, Nakhon Nayok, 26120, Thailand

[*]Corresponding Author: Nawadon Petchwattana. Email: nawadon@g.swu.ac.th

Received: 12 February 2023 Accepted: 31 March 2023 Published: 20 July 2023

ABSTRACT

Wastes from polypropylene (PP) packages are accumulating every year because it is one of the most widely consumed and short lifecycle products. This paper aims to develop low thermal conductive and fire-retardant materials from post-consumer PP (pPP) packages. Ammonium polyphosphate (APP) and hollow glass microsphere (HGM) were further added to improve the fire retardancy and thermal conductivity of pPP. The influence of APP and HGM on the mechanical and thermal properties, fire retardancy and thermal conductivity of pPP were investigated and compared with that of virgin PP (vPP). HGM was constantly added at 5 wt% while the content of APP was varied from 5 to 20 wt%. Experimental results showed that the tensile and flexural strengths were reduced with increasing APP concentrations. A morphological study confirmed the poor interfacial adhesion and debonding of each component during the applied load. Formulations containing APP less than 10 wt% did not show a satisfying fire retardancy rating due to the long self-extinguishing time. Further flame dipping and cotton ignition were observed for these formulations. With 15 and 20 wt% APP, the fire rating was significantly improved from no rating to V-0. The conductive heat transfer coefficient (k) was reduced by the presence of HGM. Based on these results, the formulation with 15 and 20 wt% could be used as a low k, fire-retardant building material.

KEYWORDS

Post-consumer polypropylene; recycling; hollow glass microsphere; thermal conductivity; fire retardancy

1 Introduction

For decades, the amount of plastic production has increased drastically due to the growth of consumption demand. This accumulates the plastic products as wastes which has drawn much environmental concern from the general public towards cleaner and greener productions [1,2].

Polypropylene (PP) is one of the most versatile petroleum-based plastics which can be applied in many value-added applications, e.g., food packaging, furniture, construction and building materials or automotive parts [3]. However, food packaging is the most widely consumed and wasted due to its short lifecycle of use. PP has massive potential for recycling due to its good mechanical strength, high thermal stability and good processability [4,5]. In 2018, the global production of PP resin was 56 Mt. Its demand is predicted to reach

88 Mt by around 2026 [6]. Based on this forecast, a large amount of PP waste is urgently needed to be utilized and managed through a circular economy.

Recycling is well-known as one of the best ways to reduce plastic waste. Generally, recycling technology can be classified into 4 categories, i.e., primary, secondary, ternary and quaternary. Primary and secondary recycling are mainly focused on re-processing and molding. However, the raw material in primary recycling is cleaner and can be processed without further washing or distinguishing the plastic types. The ternary and quaternary recycling processes are more complicated because of the complex chemical de-polymerization and pyrolysis of plastic waste, respectively [7–10]. Based on these technologies, secondary recycling seems appropriate for the waste from food packages.

There are many ways to utilize recycled polymer products, such as electronic materials from recycled face masks [11], photocatalytic materials from recycled bags and polystyrene [12], pavement materials from poly(ethylene terephthalate) (PET) bottles [13] or building materials from recycled food packages [14]. Based on these applications, recycled plastic is interesting for building materials. It requires fewer criteria for commercialization compared to those of food contact materials, cosmetic packages, electronic devices or medical devices. Numerous literatures indicated that the use of recycled PP in primary and secondary recycling did not inferiorize these properties of PP [15–17]. Thus, the use of recycled PP in building materials seems appropriate in terms of the circular economy and waste utilization issues [18–20].

In recent years, hollow glass microspheres (HGM) have been applied as a polymer additive to improve polymers' properties such as: density reduction, thermal conduction reduction and acoustic absorption [21,22]. Due to its unique and superior structure and properties, this can possibly be a good additive to pPP in terms of thermal conductivity and weight reductions for building materials application. However, the real application of building materials is widely known to face high thermal or firing conditions. The flame-retardancy function should be added to meet the requirements of building materials.

The fire-resistant material is well-known and has been used for decades, especially in polymers and polymer composites. A flame retardant based on ammonium polyphosphate (APP) was used in PP/wood composites. With 25% APP, the fire rating was raised from no rating to V-0 [23]. A synergistic flame retardance behavior was found when APP and dipentaerythritol were combined. The fire rating was improved from no rating to V-0 class with only 15.8 wt% APP [24]. Kang et al. reported the synergistic combination of HGM and intumescent flame retardant (IFR) on PP flame retardance properties. The limiting oxygen index (LOI) of pure PP was 18.0 with no fire rating. With the addition of IFR, the LOI increased to 31% and V-0. It was discovered that adding HGM to PP/IFR increased the LOI to 36.5% [25]. A combination of APP and HGM exhibited excellence in the firing and insulating properties of sodium alginate. The LOI of 100% and V-0 firing class was observed with a thermal conductivity of 0.035 W/m·K [26].

Based on the above concept, the combination of HGM and flame retardant is a possible way to improve some of the performance of post-consumer PP (pPP). Moreover, no previous work has focused on producing fire-retardant material from pPP, APP and HGM before. Thus, the current paper aims to develop fire-retardant material from pPP packages. APP and HGM were further added to improve the flame retardancy and thermal conductivity of pPP. The effects of APP and HGM on mechanical and thermal properties, flame retardancy and thermal conductivity were studied.

2 Materials and Methods

2.1 Raw Materials

The polymer matrix used in this study was the mixture of the ready-to-eat pPP packages obtained from Seven-Eleven Mini Mart at Srinakharinwirot University, Ongkharak branch. It was a mixture of 50 wt% thermoformed red and 50 wt% injection molded white PP trays as shown in Fig. 1a. The collected pPP

packages were then cleaned using washing liquid and tap water and let it dried naturally indoors. The dried samples were then ground into small pieces suitable for the extrusion process (Fig. 1b). HGM (S60) was kindly donated from 3M Co., Ltd. (Thailand), and employed as an additive for thermal conductivity and density reduction purposes. Its average particle size, thermal conductivity and true density were 30 μm, 0.208 W/(m·K) and 0.604 g/cm^3, respectively. APP was added as a fire-retardant which mainly liberated NH_3 and yielded metaphosphoric char to prevent the combustion reaction of oxygen. A virgin PP (vPP) homopolymer (POLIMAXX 1100NK, IRPC Plc, Thailand) was used as a standard material for testing and characterizations.

(a)

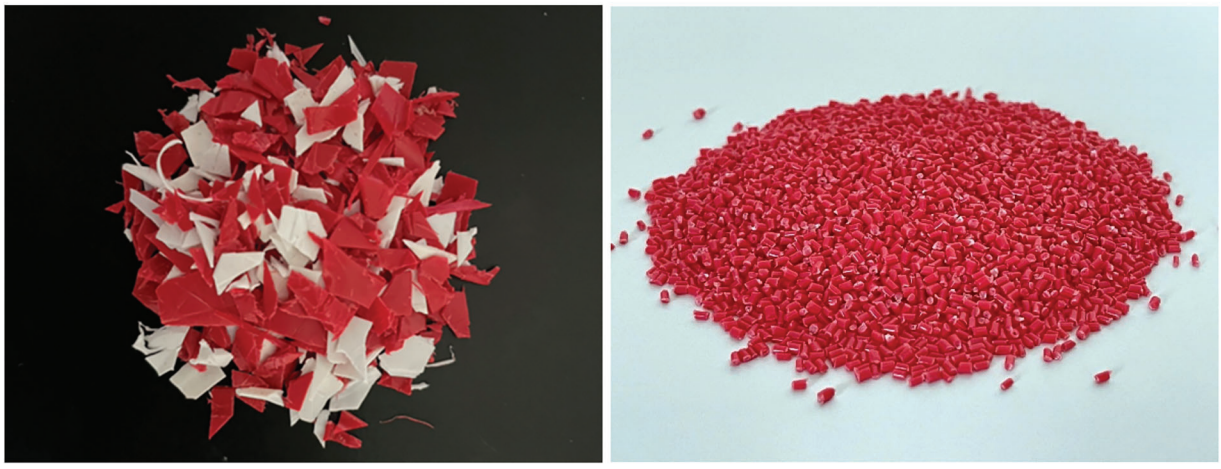

(b) (c)

Figure 1: Post-consumer PP packages used in this research (a) ready-to-eat PP packages (b) shredded PP packages and (c) pPP compound pellets

2.2 Specimens Preparation and Processing

The production process of pPP composites started with grinding pPP trays by using a blade cutting mill. The ground pPP, with a top-cut size of around 1 cm (Fig. 1b), was then dry-mixed with HGM particles and APP following the formulation shown in Table 1. Each formulation was then melt-blended using a co-rotating twin-screw extruder (Charoen Tut, CTE-D16L32, Thailand) and pelletized using a blade pelletizer (Fig. 1c). The extrusion process was operated at barrel temperatures of 175/185/195/210/195°C with a screw speed of 80–100 rpm. The extrudates were then processed using an injection molding machine (Charoen Tut, INJ101T, Thailand) for some mechanical thermal and mechanical tests as illustrated in Fig. 2. The barrel temperature of the injection process was set from 195°C, 190°C and 200°C for the back, middle and front ends, respectively. The mold temperature and the injection pressure were 45°C and 100 MPa, respectively. The total injection molding time was 60 s. Rectangular and dumbbell-shaped samples were prepared for mechanical, thermal, and morphological tests.

Table 1: Blend formulations of raw materials used included; vPP, pPP, HGM and APP

Formulation number	Formulation code	Material composition (wt%)			
		vPP	pPP	HGM	APP
1	vPP	100	–	–	–
2	pPP	–	100	–	
3	A5	–	95	–	5
4	H5A5	–	90	5	5
5	H5A10	–	85	5	10
6	H5A15	–	80	5	15
7	H5A20	–	75	5	20

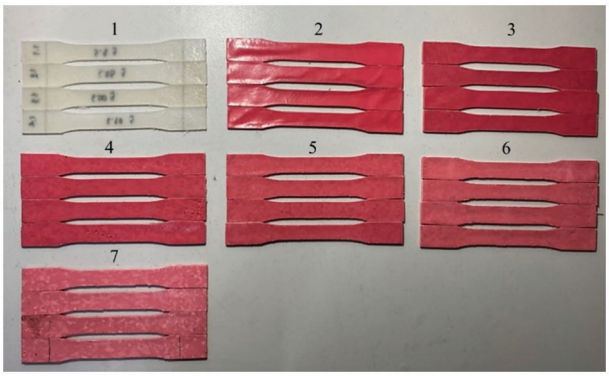

Figure 2: Visual appearance of the injection-molded vPP, pPP and pPP composites specimens corresponding to the formulation number listed in Table 1

For the thermal conductivity test, each formulation was fabricated using a compression molding machine (Charoen Tut, PR2D-W300L350-PM-WCL-HMI, Thailand). One hundred and twenty grams of the sheet were put into a 20 × 20 × 0.3 cm^3 mold and articulated with steel sheets and pre-heated for

5 min. Compression molding was processed at 190°C. A pressure of 30 bars was applied for 2 min, followed by a pressure of 100 bars for 5 min. The cooling cycle was 3 min. The final compression molded products are clearly shown in Fig. 3.

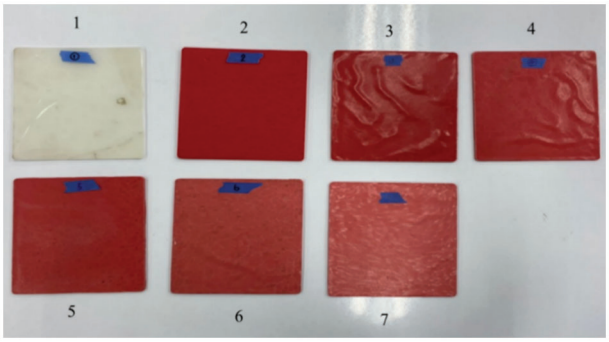

Figure 3: Visual appearance of the compression-molded specimens for the thermal conductivity test corresponding to the formulation number listed in Table 1

2.3 Testing and Characterizations

The tensile properties of vPP and pPP composites were measured in accordance with the ASTM D638 standard, using a Universal Testing Machine (Instron, 5966, USA). A gauge length of 2.54 cm and a speed of 50 mm/min were set for this test. The flexural strength was evaluated in accordance with ASTM D790 under a three-point bending mode using a Universal Testing Machine (INSTRON, 5966, USA). A support span and crosshead speed were 48 mm and 1.2 mm/min, respectively. Both flexural and tensile tests were carried out at room temperature. Five replicated samples were averaged for the tensile and flexural tests. The density of the vPP, pPP and its composites was measured by using a densimeter following the Archimedes principle.

The thermal transition behavior of vPP, pPP and pPP composites was observed using a Differential Scanning Calorimetry (DSC) technique (Perkin Elmer, DSC6000) under nitrogen condition. The test was conducted with a 10 mg sample which was firstly heated from room temperature to 220°C at a ramp rate of 10°C/min. They were then isothermally kept for 5 min and cooled down to room temperature at the identical ramp rate and held again for 5 min. Finally, they were re-heated to 220°C at 10°C/min. Data of the thermal profiles, glass transition temperature (T_g), melting temperature (T_m) and crystallization temperature (T_c) were monitored and collected. The degree of crystallinity (X_c) value was further calculated from the area under the melting peak of the second heating (Eq. (1)).

$$X_C(\%) = 100\frac{\Delta H_m}{\Delta H_f \times X_{PP}} \tag{1}$$

where ΔH_m is the enthalpy of melting obtained from the area under the melting peak. X_{PP} is the weight fraction of PP. ΔH_f is the specific heat of melting of completely crystalline PP, which is equal to 207 J/g [27].

Thermogravimetric analysis (TGA) of each formulation was measured using a Perkin Elmer Pyris 6 TGA under air atmosphere. The test was operated at a temperature range of 30–800°C at a heating rate of 10°C/min. Data of the thermal decomposition curve was reported together with the residual weight, 5% weight loss temperature (T_{D5}) and 50% weight loss temperature (T_{D50}).

The fracture morphology of vPP, pPP and pPP composites was observed using a field emission scanning electron microscope (FE-SEM) (JEOL, JSM7800F, Japan) equipped with PCSEM software. Each specimen

was fixed to an aluminum stub and coated with a conductive thin layer of gold. Each sample was tested at an acceleration voltage of 1 kV.

A vertical burning test (VB) was performed using a handmade burning chamber with the sample size of 127 × 12.7 × 3.2 mm^3 (Fig. 4). The test was operated in accordance with the UL94 standard. Data of burning time at the first (t_1) and second ignition (t_2) were recorded together with the clamp fire propagation, fire dipping and cotton ignition observation.

Figure 4: Experimental set up for the UL 94 VB test

The conductive heat transfer coefficient (k) value was estimated using a heat flow meter (NETZSCH HFM 436) which was tested using a method described in ASTMC518. Further calculation of the k value, in W/(m·K), was done by Eqs. (2) to (4):

$$q = \frac{k(T_1 - T_2)}{\Delta x} \tag{2}$$

$$R = \frac{(T_1 - T_2)}{q} \tag{3}$$

$$k = \frac{\Delta x}{R} \tag{4}$$

where q is the heat flux, in W/m^2, T_1 and T_2 are the temperature difference, Δx is the thickness of the test sample (m). R is the thermal resistance in m^2·K/W.

3 Results and Discussions

3.1 Mechanical Properties and Morphology

Table 2 shows the tensile and flexural properties of vPP, pPP and pPP composites. With 5 wt% APP (A5), the tensile strength decreased slightly compared with that of pPP. It continued to decrease with the further addition of APP and HGM. The same behavior was also found in flexural strength. This value reduced from 49.9 MPa, in pPP, to 30.1 MPa when HGM and APP were simultaneously added at 5 and 20 wt% respectively. These are because of the poor interfacial bonding between pPP, HGM and APP [28,29]. The pPP was less tough, which was reflected in the decrease in tensile elongation at break with HGM and APP loading. This is mainly due to the restriction of pPP chain entanglement from HGM and APP additions. Another reason was the PP chain scission during reprocessing which lowered its chain length and average molecular weight [30]. The tensile strength and elongation at break of poly(butylene succinate) (PBS) composites were found to be reduced with the HGM contents due to the poor interfacial adhesion and the fracture of HGM particles [29]. With the APP, both tensile strength and elongation at break were remarkably reduced due to the poor interfacial interaction. The authors suggested that the addition of silane coupling agent was found to greatly improve the dispersibility and interfacial compatibility between the APP and PP matrix [31].

Table 2: Tensile and flexural properties of vPP, pPP and pPP composites

Formulation	Tensile strength (MPa)	Tensile elongation at break (%)	Flexural strength (MPa)
vPP	36.5 ± 1.90	175 ± 6.64	42.4 ± 1.22
pPP	38.2 ± 1.46	141 ± 8.64	49.9 ± 1.57
A5	37.9 ± 1.93	95.3 ± 5.71	44.2 ± 1.92
H5A5	35.4 ± 1.36	93.5 ± 7.29	42.1 ± 1.15
H5A10	31.7 ± 1.13	64.7 ± 5.82	40.9 ± 1.26
H5A15	29.3 ± 2.67	42.1 ± 4.70	35.2 ± 1.11
H5A20	28.1 ± 1.86	37.3 ± 4.79	30.1 ± 1.68

Based on the mechanical test data, there are four possible mechanisms for pPP, HGM and APP debonding. The applied load was first applied to the pPP matrix, which resulted in matrix deformation. This load was then transferred to the rigid APP and HGM particles. These particles, however, were much more rigid than pPP. Thus, the deformation of APP and HGM particles was much lower than pPP. At this point, the pPP phase began to separate from the APP and HGM particles, resulting in debonding at the interfacial points [32].

Microscopic observation of vPP, pPP and pPP composites was clearly shown in Fig. 5. HGM showed a spherical shape while APP illustrated an asymmetry shape. In Figs. 5a and 5b, vPP showed a rougher surface compared with pPP due to its virginity. With 5 wt% APP, the pulled-out particles and the interfacial boundaries were found. This was believed to restrict the filler-matrix stress transfer, which lowered the tensile and flexural strength [3]. Some pulled-out of HGM and APP particles were found in Figs. 5d–5g. This indicated the poor interfacial bonding between pPP, APP and HGM.

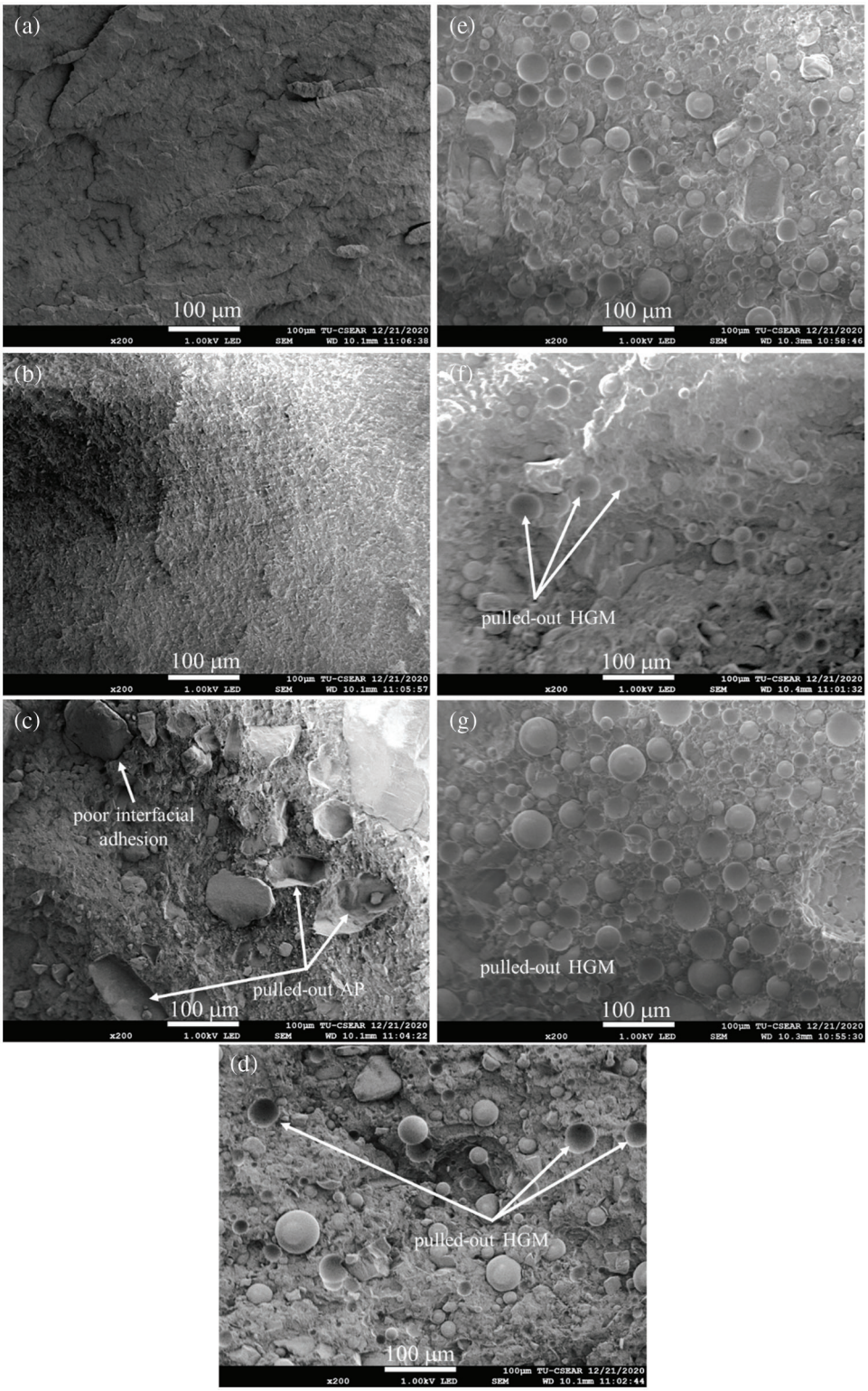

Figure 5: FE-SEM micrograph of vPP, pPP and pPP composites (a) vPP, (b) pPP, (c) A5, (d) H5A5, (e) H5A10, (f) H5A15 and (g) H5A20

3.2 Thermal and Crystallization Behaviors

Fig. 6 illustrates the DSC thermograms of vPP, pPP and pPP composites obtained from nonisothermal DSC scanning. Their corresponding T_c, T_m, ΔH_c, ΔH_m and X_c are clearly listed in Table 3. In Fig. 6a, all formulations showed identical crystallization peak characteristics of a single T_c peak. The pPP/APP and pPP/APP/HGM composites exhibited lower T_c and ΔH_c. vPP and pPP showed T_c values of 120°C and 122°C, respectively. It slightly decreased with the addition of HGM and APP by around 2°C–4°C together with the decrease of ΔH_c. This indicated the hindrance of the HGM and APP on the spherulite formation and growth under the cooling process [33].

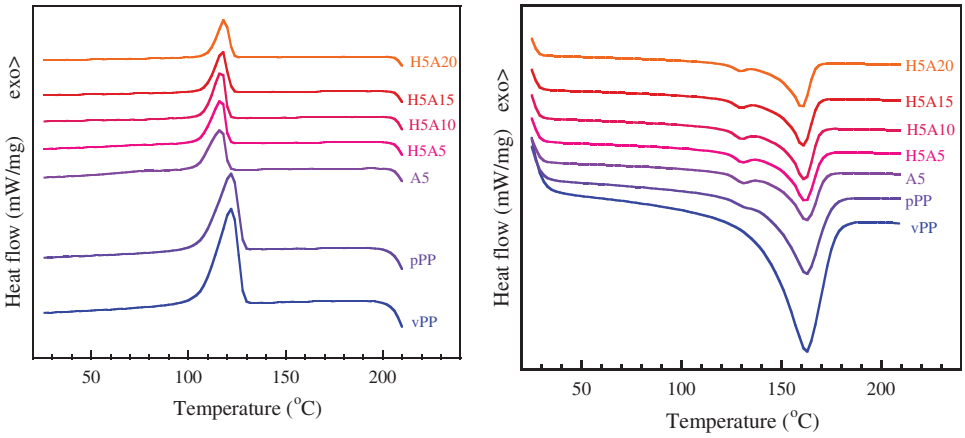

Figure 6: DSC thermogram of vPP, pPP and pPP composites (a) cooling curve and (b) 2nd heating thermogram

Table 3: Thermal transition temperature and degree of crystallinity estimated from Fig. 6

Formulation	T_c (°C)	ΔH_c (J/g)	T_m (°C)	ΔH_m (J/g)	X_c (%)
vPP	120	98.66	161	99.52	48.08
pPP	122	81.65	161	84.37	40.75
A5	118	69.58	161	65.32	33.22
H5A5	118	66.33	160	59.03	31.69
H5A10	116	62.64	159	51.57	29.31
H5A15	116	62.91	159	51.06	30.83
H5A20	116	61.39	159	47.33	30.48

In Fig. 6b, vPP showed only a single endothermic peak observed at 161°C, which corresponded to the melting of the α-crystalline phase [4,13]. For pPP, pPP/APP and pPP/APP/HGM composites, small endothermic jumps (at around 130°C) were found. For this case, it was further explained that the wasted PP was more structurally heterogeneous due to their different industrial processing and origins. Under industrial production, these products were quenched under the cooling process to reduce the production cycle time and increase productivity which induced the different crystal structures of the recycled

products [34]. The shift of the T_m peak by 1–2°C was found for all formulations compared with that of pPP and vPP. The ΔH_m and X_c were found to reduce with increasing APP concentration. This indicated that both HGM and APP obstructed pPP crystallization. X_c was found to reduce from 40.75, in pPP, to 30.48% in pPP with 20 wt% APP and 5 wt% HGM. The reduction of the X_c was previously reported in recycled PP composites with fly ash [2], wood/glass fiber mixture [9] and construction debris [10].

3.3 Decomposition Temperature

The thermal stability of vPP, pPP and pPP composites obtained from TGA is graphically presented in Fig. 7. Their corresponding onset temperature (T_{onset}), end set temperature ($T_{end\ set}$), 5% weight loss (T_{D5}) and 50% weight loss (T_{D50}) were clearly indicated in Table 4. The decomposition curve characteristic of vPP took place over a single step. It started to decompose at around 397°C and it continued decomposing with T_{D5} and T_{D50} of 407 and 452°C, respectively. The $T_{end\ set}$ and residual mass of 481°C and 0.18% were observed.

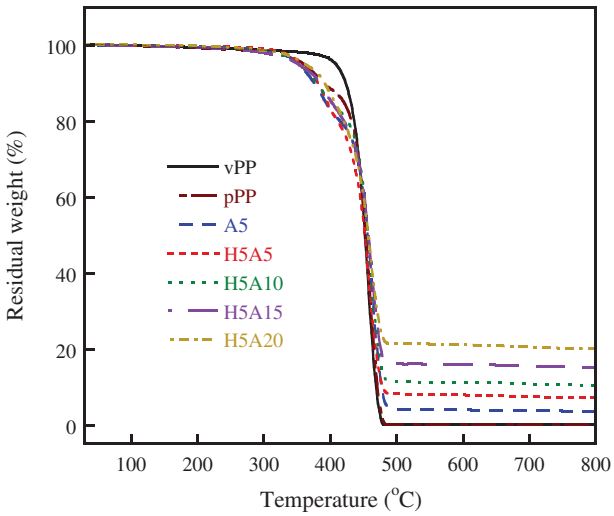

Figure 7: Thermal decomposition behavior of vPP, pPP and pPP composites

Table 4: TGA data of vPP, pPP and pPP/APP/HGM composites

Formulation	T_{onset} (°C)	T_{D5} (°C)	T_{D50} (°C)	$T_{end\ set}$ (°C)
vPP	397	408	452	481
pPP	341	404	453	481
A5	337	342	455	487
H5A5	340	346	453	488
H5A10	338	348	456	489
H5A15	336	349	457	485
H5A20	337	352	456	488

For pPP, the initial mass loss started earlier at a T_{onset} of 341°C and took place over two steps due to the decomposition of the shorter PP chain. This was the consequence of the pPP chain scission that occurred under the recycling process [35]. The second mass loss at approximately 400°C was the decomposition of the main pPP molecules. The residual mass of 0.13% was recorded at 481°C. The same decomposition behavior was observed for pPP/APP and pPP/APP/HGM composites. The T_{D50} increased slightly with increasing APP concentrations. This is mainly due to the endothermic decomposition of APP which required more heat for NH_3 gas and phosphoric acid liberations. The residual component increased with APP loading due to the residue of HGM and metaphosphoric acid resulting from APP decomposition [36] as shown in Fig. 8.

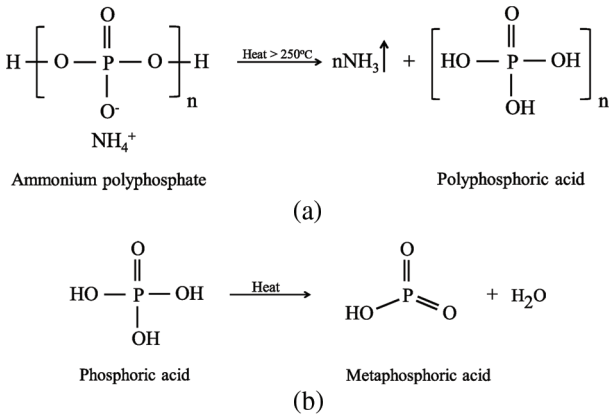

Figure 8: APP thermal decomposition reactions (a) decomposition of APP and (b) decomposition of phosphonic acid

3.4 Flame Retardancy

Table 5 shows the data from the UL94 vertical burning test. vPP and pPP showed the non-flame-retardance property due to its high burning time together with fire dripping, flaming to the clamp and cotton ignition. With the addition of APP (A5), the burning time t_2 was significantly reduced compared with that of vPP and pPP, but this value was still longer than the limitation of the UL 94 standard. A synergistic flame retardancy behavior was found when combining HGM and APP in the H5A5 formulation. This resulted in the reduction of t_2 down to 49 s. Further addition of APP to 15 and 20 wt% was found to have faster self-extinguish with V-0 classification. The achieved fire-retardance property was mainly due to the liberation of NH_3 and H_2O together with the metaphosphoric formed during combustion. This was believed to block the oxygen to contact with pPP composites [37]. A reaction of the NH_3 liberation and phosphoric acid formation was illustrated in Fig. 8a. Further decomposition of phosphoric acid released one molecule of water and metaphosphoric acid residue as shown in Fig. 8b. To improve the performance of APP, many papers recommended adding the fire retardance facilitators such as pentaerythritol derivatives, carbohydrates or spumific agents. This was previously reported to significantly improve the flame-retardancy of APP with higher char formation [31,36,38].

Table 5: Fire retardancy of vPP, pPP and pPP composites

Formulation	t_2 (s)	UL94	Dripping	Flame to clamp	Cotton ignition
vPP	186	NC	Yes	Yes	Yes
pPP	193	NC	Yes	Yes	Yes

(Continued)

Table 5 (continued)

Formulation	t_2 (s)	UL94	Dripping	Flame to clamp	Cotton ignition
A5	57	NC	Yes	No	Yes
H5A5	49	NC	No	No	No
H5A10	19	V-1	No	No	No
H5A15	7	V-0	No	No	No
H5A20	5	V-0	No	No	No

Note: NC = no classification.

3.5 Thermal Conductivity and Density

Table 6 shows the effect of HGM and APP on the *k* value of pPP. The *k* value of vPP and pPP were 0.259 and 0.262 W/(m·K), respectively, while the *k* value of HGM was 0.208 W/(m·K). Adding APP to pPP (A5) was found to slightly increase the *k* value by around 3%, which was expected based on the previous works [39,40] and the high thermal conductivity of APP. The *k* value was significantly reduced due to the presence of low conductivity HGM. The minimum value of 0.203 W/(m·K) was observed in pPP with 5wt% HGM and 5 wt% APP. However, there was an upturn of the *k* value with the increase of the APP amount. Previous reports indicated the important role of HGM in reducing the thermal conductivity of polymer composites. In low-density polyethylene (LDPE), the *k* value was found to dramatically decrease with the HGM concentrations from 0.209 W/(m·K) to 0.171 W/(m·K) for the composites with 20 wt% HGM. Further investigation on the effects of HGM diameter indicated that larger HGM was more effective in reducing the *k* value than that of smaller ones. This is due to the longer heat transfer path of the larger HGM diameter, which delayed the heat transfer rate [41].

Table 6: Conductive heat transfer coefficient and density of vPP, pPP and pPP composites

Formulation	*k* value (W/(m·K))	Density (g/cm^3)
vPP	0.259 ± 0.01	0.927 ± 0.08
pPP	0.262 ± 0.02	0.914 ± 0.04
A5	0.271 ± 0.02	0.933 ± 0.06
H5A5	0.203 ± 0.01	0.926 ± 0.02
H5A10	0.218 ± 0.01	0.971 ± 0.07
H5A15	0.225 ± 0.03	0.998 ± 0.03
H5A20	0.247 ± 0.02	1.068 ± 0.05

Based on the above result, HGM played an important role in *k* value reduction. The possible heat transfer mechanism was proposed in Fig. 9. By Assuming that all formulations were free of interfacial void or the heat transfer path was too small compared with that of HGM. The conductive heat transfer in pPP composites with HGM and APP was a combination of three possible ways. The first one was the thermal conduction by solid pPP and APP. Due to the higher *k* of APP, this may have increased the rate of heat transfer (*q*). The second was the radiation heat transfer on the surface between neighboring HGM particles. This slightly delayed the heat transfer by thermal dissipation. The last mechanism occurred through the HGM particles. In this case, the heat was transferred through the HGM wall by conduction

followed by the convection of gas in the HGM particles [42]. This was believed to be the main reason for the *k* value reduction. To maximize the HGM performance, Li et al. recommended the use of lower density HGM. They indicated that the thermal conductivity through the HGM particles was found to be significantly reduced with a reduction in HGM's true density [43].

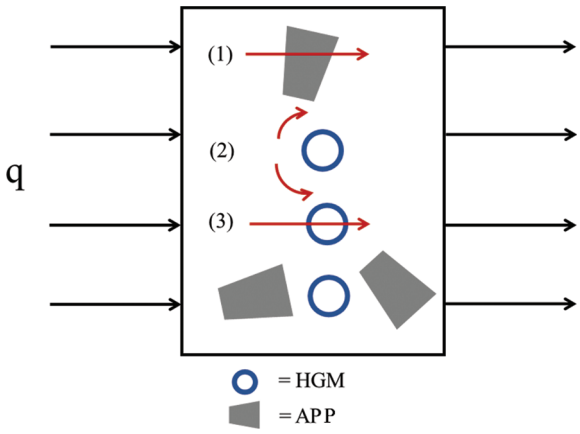

Figure 9: Possible heat transfer model of pPP/HGM/APP composites

Further observations on the density are clearly listed in Table 6. The density was found to increase with the addition of APP, but it tended to reduce with HGM addition. However, they were all higher than that of vPP and pPP. This tended to follow the rule of the mixture when the higher density APP was added. In epoxy, the density was found to reduce with the increasing volume fraction of HGM. Further comparison of the HGM wall thickness indicated that the thinner wall GHM exhibited more efficiency than that of thicker ones [44].

4 Conclusions

The low thermal conductive and fire-retardant building material was successfully prepared in this paper. Overall, the mechanical properties, including tensile strength, tensile elongation at break and flexural strength, were all reduced with the addition of HGM and APP to pPP. The morphological observation verified the poor interfacial adhesion among pPP, APP and HGM. The X_c was found to reduce with increasing APP concentrations together with the decreased T_c. The decomposition of pPP/HGM/APP composites started earlier than vPP, while the T_{D50} increased slightly. The composites containing APP less than 10 wt% did not show satisfactory flame retardancy with no fire rating combined with cotton ignition and dripping. The composites with 10, 15 and 20 wt% APP showed the V-1, V-0 and V-0 classes respectively without cotton ignition, flaming to clamp and dripping. Compared with the previous paper, adding HGM facilitated the fire-retardant property of pPP with lower APP content required. The addition of APP was found to increase the *k* value by around 3%. With the presence of HGM, the *k* value was significantly reduced with a minimum value of 0.203 W/(m·K). Based on these results, the formulation with 15 and 20 wt% could be applied as a fire-retardant building material.

Acknowledgement: The authors would like to thank the Plastic Institute of Thailand for providing of some polymer processing equipment. Thanks are extended to Miss Thitirat Piluek and Miss Sutida Khankham for the provision of waste PP packages.

Funding Statement: This research was financially supported by the Energy Conservation and Promotion Fund Office (Contract No. 014/2562) in collaboration with Thailand Science Research and Innovation (TSRI) and Srinakharinwirot University (Contract No. 034/2564).

Conflicts of Interest: The authors declare that they have no conflicts of interest to report regarding the present study.

References

1. Lai, Y. Y., Lee, Y. M. (2022). Management strategy of plastic wastes in Taiwan. *Sustainable Environment Research, 32(1),* 1–10. https://doi.org/10.1186/s42834-022-00123-0
2. Ajorloo, M., Ghodrat, M., Kang, W. H. (2021). Incorporation of recycled polypropylene and fly ash in polypropylene-based composites for automotive applications. *Journal of Polymers and the Environment, 29(4),* 1298–1309. https://doi.org/10.1007/s10924-020-01961-y
3. Petchwattana, N., Ongsritrakul, P., Covavisaruch, S., Narupai, B., Sanetuntikul, J. (2019). Polypropylene copolymer/calcium silicate composites with enhanced mechanical properties and scratch resistance. *Iranian Journal of Science and Technology, Transactions A: Science, 43(6),* 2843–2850. https://doi.org/10.1007/s40995-019-00787-1
4. Petchwattana, N., Naknaen, P., Sanetuntikul, J. (2018). Transformation of β to α phase of isotactic polypropylene nucleated with nano styrene butadiene rubber-based β-nucleating agent under microwave irradiation. *Journal of Central South University, 25(12),* 3098–3106. https://doi.org/10.1007/s11771-018-3977-3
5. Xia, T., Zhang, A., Xu, J., Chen, X., Xia, X. et al. (2021). Rheological behavior of bitumen modified by reclaimed polyethylene and polypropylene from different recycling sources. *Journal of Applied Polymer Science, 138(20),* 50435. https://doi.org/10.1002/app.50435
6. Moretti, C., Junginger, M., Shen, L. (2020). Environmental life cycle assessment of polypropylene made from used cooking oil. *Resources, Conservation and Recycling, 157(7),* 104750. https://doi.org/10.1016/j.resconrec.2020.104750
7. Datta, J., Kopczyńska, P. (2016). From polymer waste to potential main industrial products: Actual state of recycling and recovering. *Critical Reviews in Environmental Science and Technology, 46(10),* 905–946. https://doi.org/10.1080/10643389.2016.1180227
8. Lee, A., Liew, M. S. (2021). Tertiary recycling of plastics waste: an analysis of feedstock, chemical and biological degradation methods. *Journal of Material Cycles and Waste Management, 23(1),* 32–43. https://doi.org/10.1007/s10163-020-01106-2
9. Al-Maadeed, M. A., Shabana, Y. M., Khanam, P. N. (2014). Processing, characterization and modeling of recycled polypropylene/glass fibre/wood flour composites. *Materials & Design, 58(7),* 374–380. https://doi.org/10.1016/j.matdes.2014.02.044
10. Macedo, K. R. M., Cestari, S. P., Mendes, L. C., Albitres, G. A. V., Rodrigues, D. C. (2018). Sustainable hybrid composites of recycled polypropylene and construction debris. *Journal of Composite Materials, 52(21),* 2949–2959. https://doi.org/10.1177/0021998318758367
11. Mendoza, R., Oliva, J., Padmasree, K. P., Oliva, A. I., Mtz-Enriquez, A. I. et al. (2022). Highly efficient textile supercapacitors made with face masks waste and thermoelectric $Ca_3Co_4O_{9-\delta}$ oxide. *Journal of Energy Storage, 46,* 103818. https://doi.org/10.1016/j.est.2021.103818
12. Valadez-Renteria, E., Barrera-Rendon, E., Oliva, J., Rodriguez-Gonzalez, V. (2021). Flexible CuS/TiO_2 based composites made with recycled bags and polystyrene for the efficient removal of the 4-CP pesticide from drinking water. *Separation and Purification Technology, 270,* 118821. https://doi.org/10.1016/j.seppur.2021.118821
13. Panashe, J. A., Danyuo, Y. (2020). Recycling of plastic waste materials: Mechanical properties and implications for road construction. *MRS Advances, 5(25),* 1305–1312. https://doi.org/10.1557/adv.2020.197
14. Stoian, S. A., Gabor, A. R., Albu, A. M., Nicolae, C. A., Raditoiu, V. et al. (2019). Recycled polypropylene with improved thermal stability and melt processability. *Journal of Thermal Analysis and Calorimetry, 138(4),* 2469–2480. https://doi.org/10.1007/s10973-019-08824-2
15. Krause, B., Rzeczkowski, P., Pötschke, P. (2019). Thermal conductivity and electrical resistivity of melt-mixed polypropylene composites containing mixtures of carbon-based fillers. *Polymers, 11(6),* 1073. https://doi.org/10.3390/polym11061073

16. Adnan, M., Abdul-Malek, Z., Lau, K. Y., Tahir, M. (2021). Polypropylene-based nanocomposites for HVDC cable insulation. *IET Nanodielectrics, 4(3),* 84–97. https://doi.org/10.1049/nde2.12018
17. Saikrishnan, S., Jubinville, D., Tzoganakis, C., Mekonnen, T. H. (2020). Thermo-mechanical degradation of polypropylene (PP) and low-density polyethylene (LDPE) blends exposed to simulated recycling. *Polymer Degradation and Stability, 182,* 109390. https://doi.org/10.1016/j.polymdegradstab.2020.109390
18. Chen, H., Chen, Q., Xu, Y., Lawi, A. S. (2022). Effects of silica fume and fly ash on properties of mortar reinforced with recycled-polypropylene. *Construction and Building Materials, 316(18),* 125887. https://doi.org/10.1016/j.conbuildmat.2021.125887
19. Xu, S., Li, S. Y., Zhang, M., Zeng, H. Y., Wu, K. et al. (2020). Fabrication of green alginate-based and layered double hydroxides flame retardant for enhancing the fire retardancy properties of polypropylene. *Carbohydrate Polymers, 234(2),* 115891. https://doi.org/10.1016/j.carbpol.2020.115891
20. Tang, W., Song, L., Liu, F., Dessie, W., Qin, Z. et al. (2022). Improving the flame retardancy and thermal stability of polypropylene composites via introducing glycine intercalated kaolinite compounds. *Applied Clay Science, 217,* 106411. https://doi.org/10.1016/j.clay.2022.106411
21. Pakdel, E., Naebe, M., Kashi, S., Cai, Z., Xie, W. et al. (2020). Functional cotton fabric using hollow glass microspheres: Focus on thermal insulation, flame retardancy, UV-protection and acoustic performance. *Progress in Organic Coatings, 141(14),* 105553. https://doi.org/10.1016/j.porgcoat.2020.105553
22. Gogoi, R., Manik, G. (2021). Development of thermally conductive and high-specific strength polypropylene composites for thermal management applications in automotive. *Polymer Composites, 42(4),* 1945–1960. https://doi.org/10.1002/pc.25947
23. Xu, B. R., Deng, C., Li, Y. M., Lu, P., Zhao, P. P. et al. (2019). Novel amino glycerin decorated ammonium polyphosphate for the highly-efficient intumescent flame retardance of wood flour/polypropylene composite via simultaneous interfacial and bulk charring. *Composites Part B: Engineering, 172(6),* 636–648. https://doi.org/10.1016/j.compositesb.2019.05.099
24. Qin, Z., Yang, R., Zhang, W., Li, D., Jiao, Q. (2019). Synergistic barrier effect of aluminum phosphate on flame retardant polypropylene based on ammonium polyphosphate/dipentaerythritol system. *Materials & Design, 181,* 107913. https://doi.org/10.1016/j.matdes.2019.107913
25. Kang, B. H., Yang, X. Y., Lu, X. (2020). Effect of hollow glass microsphere on the flame retardancy and combustion behavior of intumescent flame retardant polypropylene composites. *Polymer Bulletin, 77(8),* 4307–4324. https://doi.org/10.1007/s00289-019-02953-2
26. Niu, Y., Wang, S., Zhu, Z., Su, M., Wang, Y. et al. (2022). Robust composite aerogels with excellent flame retardant and thermal insulation properties based on modified hollow glass microspheres. *Polymer Degradation and Stability, 202(18),* 110030. https://doi.org/10.1016/j.polymdegradstab.2022.110030
27. Rasana, N., Jayanarayanan, K., Pegoretti, A. (2018). Non-isothermal crystallization kinetics of polypropylene/short glass fibre/multiwalled carbon nanotube composites. *RSC Advances, 8(68),* 39127–39139. https://doi.org/10.1039/C8RA07243D
28. Çelebi, H. (2017). Thermal conductivity and tensile properties of hollow glass microsphere/polypropylene composites. *Anadolu University Journal of Science and Technology A–Applied Sciences and Engineering, 18(3),* 746–753. https://doi.org/10.18038/aubtda.323483
29. Petchwattana, N., Naknaen, P., Narupai, B. (2020). Crystallization behavior, mechanical, morphological and physical properties of poly(butelene succinate)/hollow glass microsphere composites: Particle size and density effects observations. *Journal of Chemical Technology and Metallurgy, 55,* 324–334.
30. Schyns, Z. O., Shaver, M. P. (2021). Mechanical recycling of packaging plastics: A review. *Macromolecular Rapid Communications, 42(3),* 2000415. https://doi.org/10.1002/marc.202000415
31. Lin, H., Yan, H., Liu, B., Wei, L., Xu, B. (2011). The influence of KH-550 on properties of ammonium polyphosphate and polypropylene flame retardant composites. *Polymer Degradation and Stability, 96(7),* 1382–1388. https://doi.org/10.1016/j.polymdegradstab.2011.03.016

32. Peng, Y., Musah, M., Via, B., Wang, X. (2021). Calcium carbonate particles filled homopolymer polypropylene at different loading levels: Mechanical properties characterization and materials failure analysis. *Journal of Composites Science, 5(11),* 302. https://doi.org/10.3390/jcs5110302
33. Ngaowthong, C., Borůvka, M., Běhálek, L., Lenfeld, P., Švec, M. et al. (2019). Recycling of sisal fiber reinforced polypropylene and polylactic acid composites: Thermo-mechanical properties, morphology, and water absorption behavior. *Waste Management, 97(5),* 71–81. https://doi.org/10.1016/j.wasman.2019.07.038
34. Baltes, L., Costiuc, L., Patachia, S., Tierean, M. (2019). Differential scanning calorimetry—a powerful tool for the determination of morphological features of the recycled polypropylene. *Journal of Thermal Analysis and Calorimetry, 138(4),* 2399–2408. https://doi.org/10.1007/s10973-019-08679-7
35. Prachayawarakorn, J., Yaembunying, N. (2005). Effect of recycling on properties of rice husk-filled-polypropylene. *Songklanakarin Journal of Science and Technology, 27(2),* 343–352.
36. Lim, K. S., Bee, S. T., Sin, L. T., Tee, T. T., Ratnam, C. T. et al. (2016). A review of application of ammonium polyphosphate as intumescent flame retardant in thermoplastic composites. *Composites Part B: Engineering, 84(5),* 155–174. https://doi.org/10.1016/j.compositesb.2015.08.066
37. Xue, D., Hu, X., Cheng, W., Yu, X., Wu, M. et al. (2020). Development of a novel composite inhibitor modified with proanthocyanidins and mixed with ammonium polyphosphate. *Energy, 213,* 118901. https://doi.org/10.1016/j.energy.2020.118901
38. Tian, N., Wen, X., Jiang, Z., Gong, J., Wang, Y. et al. (2013). Synergistic effect between a novel char forming agent and ammonium polyphosphate on flame retardancy and thermal properties of polypropylene. *Industrial & Engineering Chemistry Research, 52(32),* 10905–10915. https://doi.org/10.1021/ie401058u
39. Leng, Y., Xu, M. J., Sun, Y., Han, R. X., Li, B. (2019). Simultaneous enhancement of thermal conductivity and flame retardancy for epoxy resin thermosets through self-assemble of ammonium polyphosphate surface with graphitic carbon nitride. *Polymers for Advanced Technologies, 30(9),* 2468–2479. https://doi.org/10.1002/pat.4694
40. Liu, Y., He, J., Yang, R. (2015). Effects of dimethyl methylphosphonate, aluminum hydroxide, ammonium polyphosphate, and expandable graphite on the flame retardancy and thermal properties of polyisocyanurate-polyurethane foams. *Industrial & Engineering Chemistry Research, 54(22),* 5876–5884. https://doi.org/10.1021/acs.iecr.5b01019
41. Xing, Z., Ke, H., Wang, X., Zheng, T., Qiao, Y. et al. (2020). Investigation of the thermal conductivity of resin-based lightweight composites filled with hollow glass microspheres. *Polymers, 12(3),* 518. https://doi.org/10.3390/polym12030518
42. Li, B., Yuan, J., An, Z., Zhang, J. (2011). Effect of microstructure and physical parameters of hollow glass microsphere on insulation performance. *Materials Letters, 65(12),* 1992–1994. https://doi.org/10.1016/j.matlet.2011.03.062
43. Liang, J. Z. (2014). Estimation of thermal conductivity for polypropylene/hollow glass bead composites. *Composites Part B: Engineering, 56(1),* 431–434. https://doi.org/10.1016/j.compositesb.2013.08.072
44. Zhu, B., Ma, J., Wang, J., Wu, J., Peng, D. (2012). Thermal, dielectric and compressive properties of hollow glass microsphere filled epoxy-matrix composites. *Journal of Reinforced Plastics and Composites, 31(19),* 1311–1326. https://doi.org/10.1177/0731684412452918